Convergence Comparison of the CMA and ICA for Blind Polarization Demultiplexing

Pontus Johannisson, Henk Wymeersch, Martin Sjödin, A. Serdar Tan, Erik Agrell, Peter A. Andrekson, and Magnus Karlsson

***Abstract*—An algorithm based on independent component analysis for blind polarization demultiplexing in a coherent transmission system is presented. A comparison with the constant modulus algorithm in terms of the convergence properties is performed, and it is found that the suggested algorithm has a significantly faster convergence rate and does not have any singularity problems. We also demonstrate that the algorithm convergence is strongly dependent on the choice of starting condition and show how this can be exploited to increase the convergence rate.**

***Index Terms*—Coherent detection; Demultiplexing; Optical fiber communication; Optical fiber polarization.**

I. Introduction

Dual-polarization transmission allows for a doubling of the data rate in coherent optical transmission systems and the polarization demultiplexing at the receiver is then typically performed through digital signal processing. Several approaches are possible and, following the early attempts [1], polarization demultiplexing has been performed, for example, by channel estimation [2] and by assuming the transmitted data to be known [3]. However, for the time being, the most commonly used algorithm seems to be the constant modulus algorithm (CMA) [4]. The CMA is a blind algorithm and requires no training, but it has the drawback that the two polarization tributaries can converge to the same channel. This problem is due to the choice of cost function and requires *ad hoc* solutions [5,6]. In addition, the CMA is not designed for non-constant modulus formats such as 16 quadrature amplitude modulation (16-QAM), implying that performance improvements could be expected by using a better cost function.

Independent component analysis (ICA) is a class of algorithms for separating received linear combinations of signals [7,8]. The underlying assumption is that the transmitted signals are statistically independent. Already from this starting point it is clear that the same type of singularity that exists in the CMA cannot occur: if the two polarization tributaries converge to the same channel, then the output channels are not independent.

Although ICA is well known in the field of signal processing, its application to optical communication systems has not attracted much attention. In the first suggestion of using ICA for polarization demultiplexing by Zhang *et al.* [9], it was concluded that no singularity is present in the ICA algorithm and that the tracking performance is similar to the CMA. Another ICA approach, called *magnitude-bounded blind source separation*, has been suggested by Öktem *et al.* [10,11], and a simpler algorithm based on signal kurtosis optimization has been investigated by Xie *et al.* [12]. The algorithm presented here uses a different statistical description but otherwise similar algorithm design approach to [9]. The two other algorithms are significantly different and use other cost functions.

In this paper, an algorithm based on ICA is derived, analyzed, and the convergence properties are compared in detail to the CMA. The reason for this choice is that the CMA is well known and often used in practice. A comparison with other, previously suggested algorithms would be interesting but is outside the scope of this work. We compare with the CMA also in the case of 16-QAM, where the CMA is clearly suboptimal, since there are few alternatives. For example, the recently proposed *cascaded three-modulus algorithm* has worse convergence properties than the CMA [13] and can only be used *after* a channel estimate has been obtained. The same holds true for decision-directed algorithms, which depend on most decisions being correct. For example, the *radius-directed algorithm* [14] relies on decisions based on the amplitude, and it has been found that this algorithm does not converge well in practice [15].

Our main contributions are as follows. We have

- rigorously developed an ICA algorithm for quaternary phase-shift keying (QPSK), that, under a simplified statistical model, reverts to the algorithm in [9];
- extended this algorithm to arbitrary constellations with multiple amplitude levels;
- carried out a comparison with the CMA, based on a novel performance criterion that encapsulates the performance/latency trade-off; and
- proposed a novel method to initialize the CMA and the ICA algorithm, and quantified the resulting performance gain.

We have found that (i) contrary to [9], the suggested ICA algorithm significantly outperforms the CMA, and (ii) the

Manuscript received January 11, 2011; revised April 14, 2011; accepted April 14, 2011; published May 9, 2011 (Doc. ID 140937).

Pontus Johannisson (e-mail: pontus.johannisson@chalmers.se), Martin Sjödin, Peter A. Andrekson, and Magnus Karlsson are with the Photonics Laboratory, Department of Microtechnology and Nanoscience, Chalmers University of Technology, SE-412 96 Göteborg, Sweden.

Henk Wymeersch, A. Serdar Tan, and Erik Agrell are with the Communication Systems Group, Department of Signals and Systems, Chalmers University of Technology, SE-412 96 Göteborg, Sweden.

Digital Object Identifier 10.1364/JOCN.3.000493

choice of algorithm initial condition is critical, which can be exploited to further increase the convergence rate. The final algorithm we propose could potentially be important in a flexible optical network, where frequent rerouting of data should be expected.

The organization of this paper is as follows. In Section II, the problem is formulated and the system model is described. In Section III, the polarization demultiplexing algorithms (both CMA and ICA) are stated in detail, and the statistical description needed to apply ICA to an optical communication system is found in Section IV. The objective functions that are optimized by the algorithms are visualized for both the ICA algorithm and the CMA in Section V, leading to the discussion on the dependence on the algorithm initial condition in Section VI. In Section VII, we describe how the performance comparison of the ICA algorithm and the CMA is carried out, and finally a report of the results from numerical simulations follows in Section VIII.

Notation: Vectors are denoted in bold letters (e.g., $\mathbf{a}$), and matrices in capital bold letters (e.g., $\mathbf{A}$). Transposition is written as $\mathbf{a}^{\mathrm{T}}$, conjugation as $\mathbf{a}^{*}$, and conjugate transpose is denoted by $\mathbf{a}^{\mathrm{H}}$. The identity matrix is written as $\mathbf{I}$ and the expectation operator is denoted by $\mathbb{E}[\cdot]$.

II. Problem Formulation

We assume that chromatic dispersion has been compensated for in prior receiver components. As was also done in [9,10,12], we consider a case where polarization mode dispersion (PMD) and polarization-dependent losses (PDL) are negligible. This allows us to reduce the system complexity and focus on the fundamental task the polarization demultiplexing algorithm is designed to do—to separate the two multiplexed channels. The extension of the proposed ICA algorithm to a dispersive scenario seems straightforward, and we expect it to perform well in the presence of PMD/PDL. However, we focus on introducing the algorithm and investigating the convergence phase, and a PMD/PDL study is outside the scope of this work. Thus, we consider a system with optical amplifier noise, phase noise, and polarization mixing. An equivalent block diagram is shown in Fig. 1. At time k, the independent and identically distributed (i.i.d.) complex data symbols on the two polarizations, $\mathbf{a}_k = [a_k^{(\mathrm{X})}, a_k^{(\mathrm{Y})}]^{\mathrm{T}}$, are affected by complex additive white Gaussian noise (AWGN), $\mathbf{n}_k$, from the optical amplifiers and an unknown phase rotation, ϕ_k, due to the frequency offset of the signal and the local oscillator. The received signal phases need not be i.i.d. and can have an arbitrary distribution, possibly including symbol-by-symbol phase shifts from self-phase modulation. The sampled output is written $\mathbf{x}_k = \mathbf{A}_k \mathbf{s}_k$. The complex 2×2 matrix $\mathbf{A}_k$ is modeled as unitary, i.e., $\mathbf{A}_k^{\mathrm{H}} \mathbf{A}_k = \mathbf{I}$, and static over the observation time, which is short compared to the typical time scale of the polarization change. The goal of the polarization demultiplexing algorithm is to use the incoming stream of symbols to quickly converge to a demultiplexing matrix $\mathbf{B}_k$ and then track the polarization changes so that $\mathbf{y}_k = \mathbf{B}_k \mathbf{x}_k$ is a good estimate of $\mathbf{s}_k$.

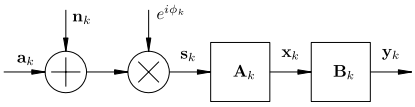

Fig. 1. System model showing the addition of noise, the phase drift, and the polarization change before the signal is sampled as $\mathbf{x}_k$.

III. Algorithm Description

For ease of reference, we start by describing the CMA, and then a description of the ICA algorithm follows.

A. The Constant Modulus Algorithm

Using the CMA [4], we minimize (w.r.t. $\mathbf{B}_k$) the cost function

$$J_{\mathrm{CMA}} = \mathbb{E}\left[(|y_k^{(\mathrm{X})}|^2 - \rho^2)^2 + (|y_k^{(\mathrm{Y})}|^2 - \rho^2)^2\right], \tag{1}$$

where $\rho^2 = \mathbb{E}[|a^{(\mathrm{X})}|^4]/\mathbb{E}[|a^{(\mathrm{X})}|^2] = \mathbb{E}[|a^{(\mathrm{Y})}|^4]/\mathbb{E}[|a^{(\mathrm{Y})}|^2]$. The corresponding stochastic gradient descent update rule is

$$\mathbf{B}_{k+1} = \mathbf{B}_k - \mu \boldsymbol{\psi}(\mathbf{y}_k)\mathbf{x}_k^{\mathrm{H}}, \tag{2}$$

where $\mu > 0$ is a step size parameter and $\boldsymbol{\psi}(\mathbf{y}_k) = (\psi^{(\mathrm{X})}, \psi^{(\mathrm{Y})})^{\mathrm{T}}$ with $\psi^{(m)}(\mathbf{y}_k) = (|y_k^{(m)}|^2 - \rho^2) y_k^{(m)}$, $m \in \{\mathrm{X}, \mathrm{Y}\}$. We observe that the CMA may converge to a singular matrix $\mathbf{B}_k$, in which the rows are identical, as this is not penalized by the cost function given in Eq. (1).

B. Independent Component Analysis

We here derive the ICA algorithm as a generalization of the result by Cardoso [8] to the case of complex random variables. Assuming that the distribution $p_{\mathbf{S}}(\mathbf{s}_k)$ at a generic time k is known and independent of k, the distribution of the received symbol, $\mathbf{x}_k = \mathbf{A}_k \mathbf{s}_k$, is [16]

$$p_{\mathbf{X}}(\mathbf{x}_k|\mathbf{A}_k) = |\det \mathbf{A}_k^{-1}|^2 \, p_{\mathbf{S}}(\mathbf{A}_k^{-1}\mathbf{x}_k). \tag{3}$$

Replacing $\mathbf{A}_k^{-1}$ with its estimate $\mathbf{B}_k$ we get

$$p_{\mathbf{X}}(\mathbf{x}_k|\mathbf{B}_k) = |\det \mathbf{B}_k|^2 \, p_{\mathbf{S}}(\mathbf{B}_k\mathbf{x}_k). \tag{4}$$

The task of the ICA algorithm is to find a matrix $\mathbf{B}_k$ such that the likelihood function given by Eq. (4) is maximized for the received samples. We obtain the log-likelihood function as

$$\Lambda(\mathbf{B}_k) = \log p_{\mathbf{X}}(\mathbf{x}_k|\mathbf{B}_k) = \log|\det \mathbf{B}_k|^2 + \log p_{\mathbf{S}}(\mathbf{y}_k). \tag{5}$$

We notice that if the $\mathbf{B}_k$ matrix is close to singular, then the determinant will be close to zero and the log-likelihood function will be low, which will avoid the singularity problem seen in the CMA.

In order to perform symbol-by-symbol stochastic steepest descent, the updating of $\mathbf{B}$ can be done according to

$$\mathbf{B}_{k+1} = \mathbf{B}_k + \mu \mathbf{G}(\mathbf{B}_k), \qquad \mathbf{G}(\mathbf{B}) = \frac{\partial \Lambda}{\partial \mathbf{B}^*}, \tag{6}$$

where μ is the step size. (This update rule is rigorously motivated by Theorem 3 in [17]. The differentiation $\partial\Lambda/\partial\mathbf{B}^*$ will yield a matrix of the same size as $\mathbf{B}$, with the (k,l) element being $\partial\Lambda/\partial B_{k,l}^*$, with $B_{k,l}$ treated as a constant [17].) A variation of this update rule, known as the *the relative gradient*, was proposed by Cardoso [8]. (It is also referred to as *the natural gradient*, introduced independently by Amari [18].) The update rule is then modified to

$$\mathbf{B}_{k+1} = \mathbf{B}_k + \mu \mathbf{G}(\mathbf{B}_k)\mathbf{B}_k^{\mathrm{H}}\mathbf{B}_k. \tag{7}$$

This leads to slightly better performance and, as shown below, simpler calculations.

As shown in Appendix A, the differentiation of the log-likelihood function yields

$$\frac{\partial \Lambda}{\partial \mathbf{B}^*} = [\mathbf{I} + \mathbf{f}(\mathbf{y})\mathbf{y}^{\mathrm{H}}]\mathbf{B}^{-\mathrm{H}}, \tag{8}$$

where

$$\mathbf{f}(\mathbf{y}) = \frac{1}{p_{\mathbf{S}}(\mathbf{y})}\frac{\partial p_{\mathbf{S}}(\mathbf{y})}{\partial \mathbf{s}^*} \tag{9}$$

and $\mathbf{B}^{-\mathrm{H}} \equiv (\mathbf{B}^{\mathrm{H}})^{-1} = (\mathbf{B}^{-1})^{\mathrm{H}}$. We notice that the inverse of $\mathbf{B}$ is canceled by the multiplication in Eq. (7), leading to a simpler expression. However, as motivated in [8], when $\mathbb{E}[\mathbf{y}\mathbf{y}^{\mathrm{H}}] = \mathbf{I}$, the $\mathbf{G}$ function can be modified to

$$\tilde{\mathbf{G}}(\mathbf{B}) = [\mathbf{I} - \mathbf{y}\mathbf{y}^{\mathrm{H}} + \mathbf{f}(\mathbf{y})\mathbf{y}^{\mathrm{H}} - \mathbf{y}\mathbf{f}(\mathbf{y})^{\mathrm{H}}]\mathbf{B}^{-\mathrm{H}}. \tag{10}$$

We have found that this change leads to a performance improvement. Equations (7), (9), and (10) together specify how to update the $\mathbf{B}$ matrix, and the next step is to describe the probability density function (PDF) $p_{\mathbf{S}}(\mathbf{s})$. This will be done in the next section.

IV. Statistical Description

Here, we find the statistical description needed to apply the ICA. First, a general derivation, which is independent of the choice of modulation format, is made to determine Eq. (9). Then, the simplifications that occur for M-ary phase-shift keying (M-PSK) are identified, and suggestions for simplifications of the general expression are given.

A. General Derivation

Without loss of generality, we assume that the phase ϕ_k contains a static component and a time-varying component. The static component is uniformly distributed in $[0, 2\pi)$ and unknown to the receiver. Thus, we first note that (i) $p_{\mathbf{S}}(\mathbf{s})$ exhibits a rotational symmetry: $p_{\mathbf{S}}(\mathbf{s}) = p_{\mathbf{S}}(\mathbf{s}e^{j\theta})$, for any θ, and (ii) $p_{\mathbf{S}}(\mathbf{s})$ does not depend on the time instant k. Second, for complexity considerations, the joint PDF $p_{\mathbf{S}}(\mathbf{s})$ will be approximated by the product of the marginal PDFs. This independence assumption gives

$$p_{\mathbf{S}}(\mathbf{s}) \approx p_S(s^{(\mathrm{X})})p_S(s^{(\mathrm{Y})}). \tag{11}$$

In order to derive an expression for the marginal PDF $p_S(s)$, we will first condition on the lth symbol, c_l, taken from an M-ary constellation, and then average over all M symbols. The corresponding s can be modeled as

$$s = (c_l + n)e^{i\phi}, \tag{12}$$

where $n \sim \mathcal{CN}(0, 2\sigma^2)$ and ϕ is a real, uniform random variable in $[0, 2\pi)$. As outlined in Appendix B, we then find the PDF to be

$$p_{S|C}(s|c_l) = \frac{1}{2\pi\sigma^2}\exp\left(-\frac{|c_l|^2 + |s|^2}{2\sigma^2}\right) I_0\left(\frac{|c_l s|}{\sigma^2}\right), \tag{13}$$

where $I_0(\cdot)$ is the 0th order modified Bessel function of the first kind. A complex random variable with this PDF has Rician modulus and uniform argument. The PDF for the entire M-point constellation in one of the polarizations is then

$$p_S(s) = \frac{1}{M}\sum_{l=1}^{M} p_{S|C}(s|c_l). \tag{14}$$

Simplifying this expression, there will be only a single term for M-PSK and a sum of three terms for rectangular 16-QAM, since $p_{S|C}(s|c_l)$ only depends on c_l through its modulus $|c_l|$. Using Eq. (14) and the assumption of independence Eq. (11), the differentiation in Eq. (9) can be performed. This allows us to find $\mathbf{f} = [f(s^{(\mathrm{X})}), f(s^{(\mathrm{Y})})]^{\mathrm{T}}$ by evaluating the function

$$f(s) = \frac{1}{2\sigma^2}\frac{\sum_{l=1}^{M} p_{S|C}(s|c_l)\left[\frac{I_1(|c_l s|/\sigma^2)}{I_0(|c_l s|/\sigma^2)}|c_l|e^{i\angle s} - s\right]}{\sum_{l=1}^{M} p_{S|C}(s|c_l)}. \tag{15}$$

B. Simplifications and Approximations

Equation (15) is general and can be used for any modulation format. However, the expression for $\mathbf{f}$ is quite complicated, and exponential and Bessel functions may be difficult to use in a real-time optical receiver. It is therefore necessary to simplify the expressions. For M-PSK, significant simplification occurs automatically since there is only one amplitude level and the PDF function in Eq. (15) cancels out. Furthermore, at realistic signal to noise ratio (SNR) levels, the ratio I_1/I_0 is typically close to unity. It is reasonable to replace the ratio with a constant value by evaluating it at the symbol amplitude to get

$$f_{M\text{-PSK}}(s) \approx \frac{1}{2\sigma^2}(D|c_1|e^{i\angle s} - s), \tag{16}$$

$$D = \frac{I_1(|c_1|^2/\sigma^2)}{I_0(|c_1|^2/\sigma^2)}. \tag{17}$$

As discussed in [19], the CMA needs 16 complex multiplications per update while the ICA algorithm needs 22 complex

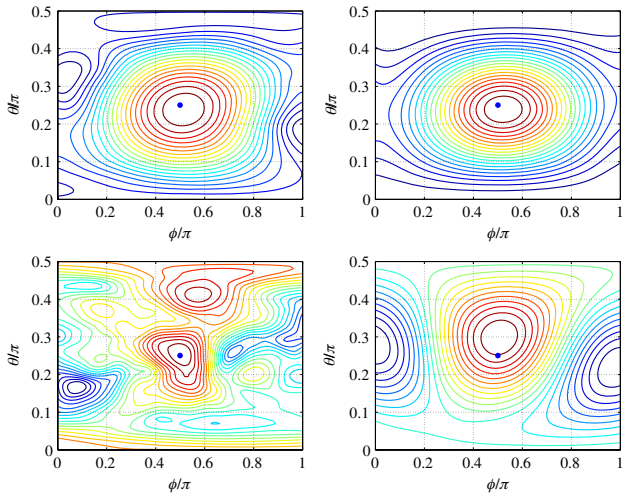

Fig. 2. (Color online) Contour plots of the objective functions Λ and J_{CMA}. Top row: QPSK. Bottom row: 16-QAM. Left column: ICA. Right column: CMA. The solution is indicated by the dot.

multiplications and 2 phase extractions per update. When using QPSK, the increase in computational complexity for the ICA algorithm is therefore small compared to the CMA.

For modulation formats with more than one amplitude level (such as 16-QAM), we see from Eq. (15) that $\mathbf{f}$ will be a sum of terms weighted by the PDF. One possible approximation is to replace this sum with a single term, by choosing the one that has the largest weight. Apart from one decision based on the $\mathbf{y}$ value, the computational complexity is then the same as for the M-PSK case. Preliminary simulations have shown that the impact from such an approximation is quite limited, but a detailed trade-off analysis is outside the scope of this work.

V. Visualization of the Optimization Problem

The optimization by steepest descent is done, in the case of the ICA algorithm, with the log-likelihood function Λ, and, in the case of the CMA, with the cost function J_{CMA}. By plotting these objective functions for a set of trial demultiplexing matrices, we can gain some valuable insight into the performance properties of the different algorithms. However, the $\mathbf{A}$ matrix has four degrees of freedom, since it can be written as

$$\mathbf{A} = \begin{pmatrix} u & v \\ -v^* & u^* \end{pmatrix} e^{i\phi_{\mathrm{common}}} \tag{18}$$

with $|u|^2 + |v|^2 = 1$. This four-dimensional set of matrices is hard to visualize, but the fact that a phase rotation of the X and Y channels is of no consequence (since it will be dealt with in the subsequent phase synchronization) means that we can use a demultiplexing matrix of the form

$$\mathbf{B}(\theta,\phi) = \begin{pmatrix} \cos\theta & \sin\theta e^{i\phi} \\ -\sin\theta e^{-i\phi} & \cos\theta \end{pmatrix}. \tag{19}$$

This is easy to prove by introducing a matrix

$$\mathbf{V} = \begin{pmatrix} e^{i\eta^{(\mathrm{X})}} & 0 \\ 0 & e^{i\eta^{(\mathrm{Y})}} \end{pmatrix}, \tag{20}$$

which simply rotates the X and Y channels individually. It is then always possible to find θ, ϕ, $\eta^{(\mathrm{X})}$, and $\eta^{(\mathrm{Y})}$, so that $\mathbf{VBA} = \mathbf{I}$ is fulfilled.

A further reduction of the parameter space is obtained by noticing that if one demultiplexing matrix $\mathbf{B}(\theta,\phi)$ has been found, then $\mathbf{B}(\theta+\pi/2,\phi)$ and $\mathbf{B}(-\theta+\pi/2,\phi+\pi)$ are also demultiplexing matrices. (This will introduce phase shifts and/or swap the two channels, but neither is of consequence for the demultiplexing task.) Thus, there is always one solution in $\theta \in [0,\pi/2)$ and $\phi \in [0,\pi)$.

By generating a number of random data symbols according to the system model, we can plot the objective function as a function of θ and ϕ. Using a large number of data symbols, the objective functions become similar for the ICA algorithm and the CMA using both QPSK and 16-QAM. (The only qualitative difference is that in the case of the ICA algorithm and 16-QAM, the objective function has a slightly narrower peak around the correct value.) It is of more interest, therefore, to visualize the situation when only a small number of symbols are used to estimate the demultiplexing matrix. Therefore, the objective functions have been plotted using only 20 symbols in Fig. 2, which makes the difference between the algorithms clearly visible. The $\mathbf{A}$ matrix has been chosen to be $\mathbf{B}(\pi/4,\pi/2)^{-1}$, the sign of J_{CMA} has been changed to make the two plots more visually similar, and a common set of symbols is used for both the ICA algorithm and the CMA to obtain a fair comparison. The details of these figures vary depending on the specific realization of random data, but the case shown is typical.

In the case of QPSK (top row), both the ICA algorithm and the CMA will position the optimum close to the true value. Some deviation from the true case is seen, since the innermost contour is slightly elliptical and offset a small distance from the true value. It is not possible to draw any qualitative conclusions about the QPSK performance differences of the ICA algorithm and the CMA, but the fact that 16-QAM leads to a significantly harder problem is well illustrated in the bottom row. This fact is, however, manifested in quite different ways for the ICA algorithm and the CMA. In the ICA case, the objective function has a complex appearance, but the global optimum is still located close to the true value, showing that a good estimation of the demultiplexing matrix should be possible. In the case of the CMA, the objective function remains qualitatively similar to the QPSK case, but the optimum is typically offset a larger distance from the true value. This suggests the conclusion that, if the demultiplexing matrix is reasonably close to the solution, then the ICA algorithm should be capable of estimating the objective function gradient better than the CMA for 16-QAM. This would correspond to faster convergence and better tracking performance, which agrees with our numerical results in Section VIII.

VI. Choice of Initial Matrix

As shown in Section V, the objective function for the ICA algorithm in the 16-QAM case is "bumpy" when estimated from a small number of symbols. We therefore anticipate that, if the initial matrix happens to be chosen in an area corresponding to demultiplexing matrices that are far from the solution, then the convergence will be slow. A remedy for this would be to make sure that such cases are avoided, and this can be done in (at least) two ways: either we select the initial matrix by evaluating the objective function for a set of candidate matrices or we perform the computation for a number of different initial matrices in parallel and then select the best solution at a later stage. Here, "best" refers to the matrix that corresponds to the lowest cost/maximum log-likelihood. The first method would require the evaluation of the objective function on a number of symbols (as done in the previous section) and has the disadvantage that the iteration by steepest descent cannot be started until the initial matrix has been selected. Here, we have investigated the second suggestion, which is more computationally demanding but is easy to parallelize since the computations are completely independent. We carefully notice that such a scheme can be used to improve the convergence rate regardless of the choice of algorithm. We have therefore carried out numerical simulations using this method for both the ICA algorithm and the CMA.

The question of how to select an arbitrary number of initial matrices in such a way as to maximize the convergence rate is non-trivial. We leave this issue for later study and only present the results for the following case. Considering the periodicity stated in Section V, it is reasonable to generate a set of initial matrices by dividing the parameter space into a 2×2 grid, yielding $\mathbf{B}(0,0)$, $\mathbf{B}(\pi/4,0)$, $\mathbf{B}(0,\pi/2)$, and $\mathbf{B}(\pi/4,\pi/2)$. However, $\mathbf{B}(0,0)=\mathbf{B}(0,\pi/2)$, so we can discard the latter. The remaining set of three initial matrices is reasonable, but we do not claim it to be an optimal choice. Starting from these three matrices we perform the computation in parallel and the results are presented in Subsection VIII.B.

VII. Comparing the ICA Algorithm and the CMA

In order to compare the ICA algorithm and the CMA in a fair manner, a good performance measure needs to be defined. The most relevant measure is the bit error rate (BER). This is possible to use, since the system is entirely known at every update of the $\mathbf{B}$ matrix, but it is quite computationally demanding. An alternative way, which is directly related to the BER, is to use the SNR penalty due to the imperfect polarization demultiplexing. We will use this as the criterion for comparing the two algorithms.

The SNR penalty is calculated in the following way. Defining $\mathbf{C}=\mathbf{BA}$, we have $\mathbf{y}=\mathbf{Cs}=\mathbf{C}(\mathbf{a}+\mathbf{n})e^{i\phi}$, or

$$\begin{pmatrix} y^{(\mathrm{X})} \\ y^{(\mathrm{Y})} \end{pmatrix} = \begin{pmatrix} C_{11} & C_{12} \\ C_{21} & C_{22} \end{pmatrix} \begin{pmatrix} a^{(\mathrm{X})}+n^{(\mathrm{X})} \\ a^{(\mathrm{Y})}+n^{(\mathrm{Y})} \end{pmatrix} e^{i\phi}. \tag{21}$$

Assuming $|C_{11}||C_{22}|>|C_{12}||C_{21}|$, we can view the $a^{(\mathrm{Y})}$-term in $y^{(\mathrm{X})}$ as part of the noise to obtain

$$\mathrm{SNR}^{(\mathrm{X})} = \frac{\mathbb{E}\left[|C_{11}a^{(\mathrm{X})}|^2\right]}{\mathbb{E}\left[|C_{11}n^{(\mathrm{X})}+C_{12}a^{(\mathrm{Y})}+C_{12}n^{(\mathrm{Y})}|^2\right]}, \tag{22}$$

which, when simplified, yields

$$\mathrm{SNR}^{(\mathrm{X})} = \frac{|C_{11}|^2E_s}{|C_{12}|^2E_s+2\sigma^2(|C_{11}|^2+|C_{12}|^2)}, \tag{23}$$

where $E_s=\mathbb{E}\left[|a^{(\mathrm{X})}|^2\right]=\mathbb{E}\left[|a^{(\mathrm{Y})}|^2\right]$. We notice that for perfect demultiplexing, i.e., for $C_{12}=0$, we recover the nominal $\mathrm{SNR}^{\mathrm{nom}}=E_s/(2\sigma^2)$. The expression for $\mathrm{SNR}^{(\mathrm{Y})}$ is obtained in an analogous manner, and we define the SNR penalty at iteration k as

$$\mathrm{SNR}_k^{\mathrm{pen}} = \mathrm{SNR}^{\mathrm{nom}} - \min(\mathrm{SNR}_k^{(\mathrm{X})}, \mathrm{SNR}_k^{(\mathrm{Y})}), \tag{24}$$

where we assume all SNR values to be given in dB.

There is one detail that must be resolved to use this method: no demultiplexing algorithm is able to avoid the possibility of channel swapping, since the two channels are identical in every statistical sense (without the introduction of training sequences or similar asymmetry) [8]. Thus, if $|C_{11}||C_{22}|<|C_{12}||C_{21}|$, then the rows of the $\mathbf{C}$ matrix are swapped before the SNR penalty is calculated.

VIII. Numerical Simulations

Numerical simulations have been performed to compare the convergence rates of the CMA and the ICA algorithm, both without (Subsection VIII.A) and with (Subsection VIII.B) the parallel approach. For the CMA, the updating of the $\mathbf{B}$ matrix is done according to Eq. (2). For the ICA algorithm the update rule defined by Eq. (7) has been used together with the exact PDF found in Section IV. The $\mathbf{A}$ matrix is drawn uniformly from the set of 2×2 unitary matrices, and is then held constant during the simulation. This is reasonable for limited observation times, say, 2000 symbols, as this corresponds to 0.2 μs at 10 Gbaud, which is too short a time to have any significant changes of the polarization state. A symbol sequence is generated and complex AWGN is added, corresponding to a nominal BER of 10^{-3}. By running a large number of simulations using different $\mathbf{A}$ matrices, we can compute the probability of being above a given SNR penalty threshold at every iteration. (This is possible since the SNR penalty can be computed using the $\mathbf{B}_k$ matrix and the expressions in the previous section.) We have set the convergence threshold value to be 1 dB SNR penalty and used the probabilities found as a measure of the convergence rate.

The step size μ must be chosen in every individual case since it affects the computed probabilities. In all cases, the step size has been selected to maximize the final probability of being below 1 dB penalty.

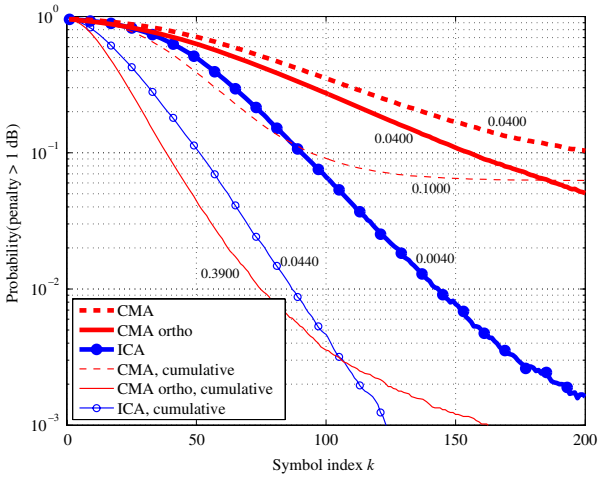

Fig. 3. (Color online) Probability for being above 1 dB penalty for the CMA and the ICA algorithm on 200 symbols of QPSK data. The thick lines are symbol-by-symbol updates and the thin lines use the cumulative approach. The step size, μ, is indicated next to each curve.

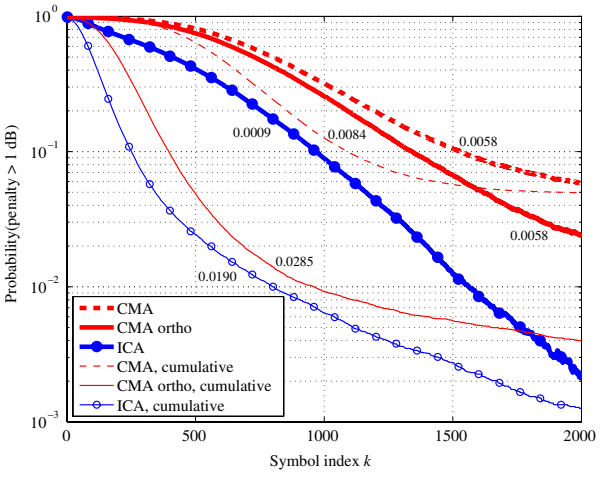

Fig. 4. (Color online) Probability for being above 1 dB penalty for the CMA and the ICA algorithm on 2000 symbols of 16-QAM data. The thick lines are symbol-by-symbol updates and the thin lines use the cumulative approach. The step size, μ, is indicated next to each curve.

A. Symbol-by-Symbol and Cumulative Updates

Figures 3 and 4 show results for QPSK and 16-QAM, respectively, with the initial estimate of $\mathbf{B}$ set to $\mathbf{I}$. The thick lines correspond to symbol-by-symbol updates, where the gradient in every iteration is estimated from a single symbol. The thin lines show cumulative updates, where at time k we perform a gradient descent based on all the observed symbols up to time k. This cumulative approach has high computational complexity, but is included to show the achievable performance by making use of all available information in every time step.

For the symbol-by-symbol updates, the ICA algorithm is used for the blue line marked with circles and the CMA is used for the two red lines. The solid line for the CMA corresponds to an implementation suggested by Kikuchi [5], which avoids the singularity problem by orthogonalizing the rows of $\mathbf{B}_k$ in every time step. We have included this algorithm in the comparison, since Kikuchi's algorithm is very similar to the conventional CMA but achieves singularity-free operation with minimal changes. Other approaches have been suggested to avoid the singularity. For example, algorithms that force the demultiplexing matrix to be unitary are discussed in [20,21]. However, a comprehensive comparison of algorithms is outside the scope of this work. It is seen that the ICA algorithm outperforms the CMA for both modulation formats, since it has a significantly lower probability of being above the SNR penalty threshold. We also notice that it is not the singularity problem that is causing the relatively low convergence rate of the CMA. This shows that the ICA algorithm is much more efficient in estimating the polarization state from a given set of data. However, in the 16-QAM case, the probability for being above 1 dB penalty is more than 10^{-3} for both algorithms also after 2000 symbols. This problem is related to the observations made in Section V; the CMA cost function is not designed for 16-QAM and the ICA objective function is no longer smooth, leading to slower convergence toward the minimum.

For the cumulative updates, the simulation results are shown using thin lines in Figs. 3 and 4. Particularly striking is the improvement for the CMA in the QPSK case, showing that basing the gradient estimate on more than one symbol has the potential of increasing the convergence rate considerably. This improvement must, however, be weighed against the increased computational complexity.

B. Convergence Improvements From Parallelization

From Figs. 3 and 4, we notice a tendency for several of the curves to start to level out for increasing k. In general, it should be expected that for a given step size, the curve will level out at a corresponding probability value. This is because in the converged state there is still a finite probability that the matrix leaves the allowed 1 dB penalty region. Thus, there is a limit on how quickly low failure probabilities can be obtained by increasing the step size. As described in Section VI, we have investigated how further convergence rate improvements can be obtained by running three independent computations in parallel using a set of initial matrices.

The numerical results are shown in Figs. 5 and 6 for the CMA (red) and the ICA algorithm (blue with circles). The thick lines are the individual symbol-by-symbol results, which should become identical if averaged over a very large number of invocations. (This is true since all initial guesses are equally good.) Corresponding lines are also found in Figs. 3 and 4, but the step sizes are reduced here to avoid the combined result leveling out above the 10^{-3} level. The thin lines have been generated by selecting the matrix corresponding to the lowest cost/maximum log-likelihood in every iteration (based on all previous symbols).

It is seen that the speedup of the convergence rate is substantial for both algorithms and both modulation formats. The ICA algorithm has a speed advantage over the CMA of more than a factor of two in reaching the 10^{-3} level, but

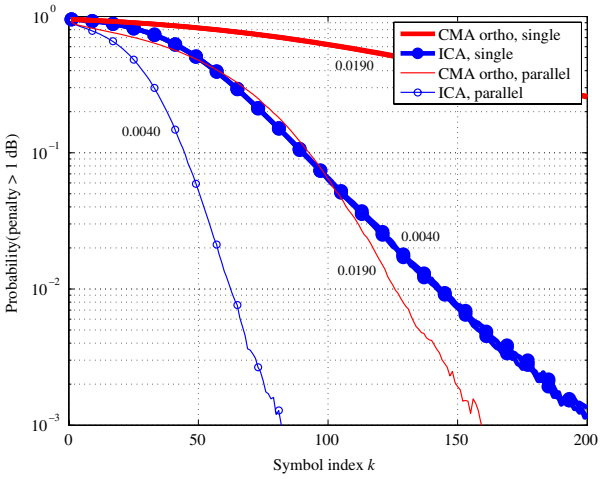

Fig. 5. (Color online) Probability for being above 1 dB penalty for the CMA and the ICA algorithm on 200 symbols of QPSK data. The thick lines show three parallel runs and the thin lines show the combined result. The step size, μ, is indicated next to each curve.

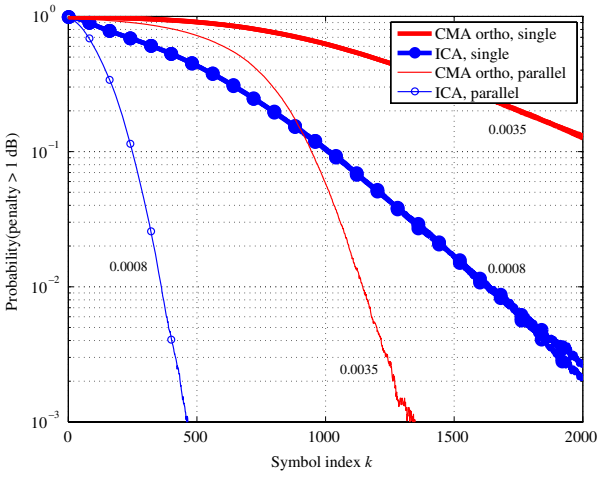

Fig. 6. (Color online) Probability for being above 1 dB penalty for the CMA and the ICA algorithm on 2000 symbols of 16-QAM data. The thick lines show three parallel runs and the thin lines show the combined result. The step size, μ, is indicated next to each curve.

if the CMA is preferred for its simplicity, then a careful selection of the initial matrix would lead to significantly better convergence properties.

Comparing this result to the cumulative approach above, we conclude that the performance improvement from using a better estimate of the gradient is small compared to the larger gains that can be achieved in this way. Thus, the choice of initial matrix is very important for the convergence rate of the polarization demultiplexing algorithm.

IX. Conclusion

We have compared the constant modulus algorithm and independent component analysis for polarization demultiplexing in terms of their convergence rates. It was found that, for a given number of symbols and a set SNR penalty limit, the ICA algorithm has a significantly lower probability of failure. It was further shown that the choice of the initial matrix is very important for the algorithm performance and that substantial improvement of the convergence rate can be obtained by running a number of parallel independent computations starting from different initial matrices.

Appendix A: Differentiation of the Log-Likelihood Function

In order to differentiate the log-likelihood function in Eq. (5), we rewrite

$$\log|\det\mathbf{B}|^2 = \log\det(\mathbf{B}\mathbf{B}^*), \tag{25}$$

and, using [22], we find the result

$$\frac{\partial}{\partial\mathbf{B}^*}\log|\det\mathbf{B}|^2 = \mathbf{B}^{-\mathrm{H}}. \tag{26}$$

For the remaining part of the expression, we need the chain rule for complex-valued functions of matrices [22], which says that, if

$$\mathbf{H}(\mathbf{Z},\mathbf{Z}^*) = \mathbf{G}(\mathbf{F}(\mathbf{Z},\mathbf{Z}^*),\mathbf{F}^*(\mathbf{Z},\mathbf{Z}^*)), \tag{27}$$

then the derivative of the matrix function $\mathbf{H}(\mathbf{Z},\mathbf{Z}^*)$ with respect to $\mathbf{Z}^*$ is

$$\mathscr{D}_{\mathbf{Z}^*}\mathbf{H} = (\mathscr{D}_{\mathbf{F}}\mathbf{G})(\mathscr{D}_{\mathbf{Z}^*}\mathbf{F}) + (\mathscr{D}_{\mathbf{F}^*}\mathbf{G})(\mathscr{D}_{\mathbf{Z}^*}\mathbf{F}^*). \tag{28}$$

This directly gives us

$$\begin{aligned}\frac{\partial p_{\mathbf{S}}(\mathbf{B}\mathbf{x})}{\partial\mathbf{B}^*} &= \frac{\partial p_{\mathbf{S}}(\mathbf{B}\mathbf{x})}{\partial\mathbf{s}}\underbrace{\frac{\partial(\mathbf{B}\mathbf{x})}{\partial\mathbf{B}^*}}_{=0} + \frac{\partial p_{\mathbf{S}}(\mathbf{B}\mathbf{x})}{\partial\mathbf{s}^*}\frac{\partial(\mathbf{B}\mathbf{x})^*}{\partial\mathbf{B}^*}\\ &= \frac{\partial p_{\mathbf{S}}(\mathbf{B}\mathbf{x})}{\partial\mathbf{s}^*}\mathbf{x}^{\mathrm{H}} = \frac{\partial p_{\mathbf{S}}(\mathbf{y})}{\partial\mathbf{s}^*}\mathbf{y}^{\mathrm{H}}\mathbf{B}^{-\mathrm{H}},\end{aligned} \tag{29}$$

where it was used that $\mathbf{y} = \mathbf{B}\mathbf{x}$. (One easy way to check this is to calculate $\partial p_{\mathbf{S}}/\partial B_{11}^*$, etc.) This gives us the final result

$$\frac{\partial\Lambda}{\partial\mathbf{B}^*} = \left[\mathbf{I} + \frac{1}{p_{\mathbf{S}}(\mathbf{y})}\frac{\partial p_{\mathbf{S}}(\mathbf{y})}{\partial\mathbf{s}^*}\mathbf{y}^{\mathrm{H}}\right]\mathbf{B}^{-\mathrm{H}}. \tag{30}$$

Appendix B: Derivation of the Exact PDF

In order to derive the PDF given in Eq. (13), we study the expression

$$S = (a + X)e^{i\Phi}, \tag{31}$$

where a is a complex constant, X is described by the PDF

$$p_X(x) = \frac{1}{2\pi\sigma^2}\exp\left(-\frac{|x|^2}{2\sigma^2}\right), \tag{32}$$

and Φ is a real, uniform random variable in $[0,2\pi)$. Writing this as

$$X = Se^{-i\Phi} - a, \tag{33}$$

we identify the conditional PDF for a given Φ to be

$$p_{S|\Phi,A}(s|\phi,a) = \frac{1}{2\pi\sigma^2}\exp\left(-\frac{|se^{-i\phi}-a|^2}{2\sigma^2}\right). \tag{34}$$

Thus, we find the sought PDF as

$$\begin{aligned} p_{S|A}(s|a) &= \int_0^{2\pi} p_{S|\Phi,A}(s|\phi,a)p_\Phi(\phi)d\phi \\ &= \frac{1}{4\pi^2\sigma^2}\exp\left(-\frac{|a|^2+|s|^2}{2\sigma^2}\right)f\left(\frac{a^*s}{\sigma^2}\right), \end{aligned} \tag{35}$$

where

$$f(\xi) \equiv \int_0^{2\pi} \exp[\mathrm{Re}(\xi e^{-i\phi})]d\phi. \tag{36}$$

Writing this as

$$f(\xi) = \int_0^{2\pi} \exp\left\{|\xi|\mathrm{Re}\left[e^{i(\angle\xi-\phi)}\right]\right\}d\phi, \tag{37}$$

we can easily find the result

$$f(\xi) = 2\pi I_0(|\xi|), \tag{38}$$

where $I_0(\cdot)$ is the 0th order modified Bessel function of the first kind.

ACKNOWLEDGMENT

This work was supported in part by the Swedish Governmental Agency for Innovation Systems (VINNOVA) and the EU EURO-FOS project.

REFERENCES

[1] M. Tseytlin, O. Ritterbush, and A. Salamon, "Digital, endless polarization control for polarization multiplexed fiber-optic communications," in *Optical Fiber Communication Conf. (OFC)*, 2003, MF83.

[2] R. Noé, "PLL-free synchronous QPSK polarization multiplex/diversity receiver concept with digital I&Q baseband processing," *IEEE Photon. Technol. Lett.*, vol. 17, no. 4, pp. 887–889, Apr. 2005.

[3] Y. Han and G. Li, "Coherent optical communication using polarization multiple-input–multiple-output," *Opt. Express*, vol. 13, no. 19, pp. 7527–7534, Sept. 2005.

[4] D. N. Godard, "Self-recovering equalization and carrier tracking in two-dimensional data communication systems," *IEEE Trans. Commun.*, vol. 28, no. 11, pp. 1867–1875, Nov. 1980.

[5] K. Kikuchi, "Polarization-demultiplexing algorithm in the digital coherent receiver," in *IEEE/LEOS Summer Topical Meetings (LEOSST)*, 2008, MC2.2.

[6] L. Liu, Z. Tao, W. Yan, S. Oda, T. Hoshida, and J. C. Rasmussen, "Initial tap setup of constant modulus algorithm for polarization de-multiplexing in optical coherent receivers," in *Optical Fiber Communication Conf. (OFC)*, 2009, OMT2.

[7] J.-F. Cardoso and B. H. Laheld, "Equivariant adaptive source separation," *IEEE Trans. Signal Process.*, vol. 44, no. 12, pp. 3017–3030, Dec. 1996.

[8] J.-F. Cardoso, "Blind signal separation: statistical principles," *Proc. IEEE*, vol. 86, no. 10, pp. 2009–2025, Oct. 1998.

[9] H. Zhang, Z. Tao, L. Liu, S. Oda, T. Hoshida, and J. C. Rasmussen, "Polarization demultiplexing based on independent component analysis in optical coherent receivers," in *European Conf. Optical Communication (ECOC)*, 2008, Mo.3.D.5.

[10] T. Öktem, A. T. Erdogan, and A. Demir, "Adaptive receiver structures for fiber communication systems employing polarization-division multiplexing," *J. Lightwave Technol.*, vol. 27, no. 23, pp. 5394–5404, Dec. 2009.

[11] T. Öktem, A. T. Erdogan, and A. Demir, "Adaptive receiver structures for fiber communication systems employing polarization division multiplexing: high symbol rate case," *J. Lightwave Technol.*, vol. 28, no. 10, pp. 1536–1546, May 2010.

[12] X. Xie, F. Yaman, X. Zhou, and G. Li, "Polarization demultiplexing by independent component analysis," *IEEE Photon. Technol. Lett.*, vol. 22, no. 11, pp. 805–807, June 2010.

[13] X. Zhou and J. Yu, "200-Gb/s PDM-16QAM generation using a new synthesizing method," in *European Conf. Optical Communication (ECOC)*, 2009, 10.3.5.

[14] I. Fatadin, D. Ives, and S. J. Savory, "Blind equalization and carrier phase recovery in a 16-QAM optical coherent system," *J. Lightwave Technol.*, vol. 27, no. 15, pp. 3042–3049, Aug. 2009.

[15] P. J. Winzer, A. H. Gnauck, C. R. Doerr, M. Magarini, and L. L. Buhl, "Spectrally efficient long-haul optical networking using 112-Gb/s polarization-multiplexed 16-QAM," *J. Lightwave Technol.*, vol. 28, no. 4, pp. 547–556, Feb. 2010.

[16] P. J. Schreier and L. L. Scharf, *Statistical Signal Processing of Complex-Valued Data*, Cambridge University Press, 2010.

[17] A. Hjørungnes and D. Gesbert, "Complex-valued matrix differentiation: techniques and key results," *IEEE Trans. Signal Process.*, vol. 55, no. 6, pp. 2740–2746, June 2007.

[18] S. Amari, "Natural gradient works efficiently in learning," *Neural Comput.*, vol. 10, no. 2, pp. 251–276, Feb. 1998.

[19] P. Johannisson, H. Wymeersch, M. Sjödin, A. S. Tan, E. Agrell, P. A. Andrekson, and M. Karlsson, "Convergence comparison of CMA and ICA for blind polarization demultiplexing of QPSK and 16-QAM signals," in *European Conf. Optical Communication (ECOC)*, 2010, Th.9.A.3.

[20] I. Roudas, A. Vgenis, C. S. Petrou, D. Toumpakaris, J. Hurley, M. Sauer, J. Downie, Y. Mauro, and S. Raghavan, "Optimal polarization demultiplexing for coherent optical communications systems," *J. Lightwave Technol.*, vol. 28, no. 7, pp. 1121–1134, Apr. 2010.

[21] S. J. Savory, "Digital coherent optical receivers: Algorithms and subsystems," *IEEE J. Sel. Top. Quantum Electron.*, vol. 16, no. 5, pp. 1164–1179, Sept./Oct. 2010.

[22] A. Hjørungnes, D. Gesbert, and D. P. Palomar, "Unified theory of complex-valued matrix differentiation," in *IEEE Int. Conf. Acoustics, Speech and Signal Processing*, 2007, vol. 3.

Pontus Johannisson received his Ph.D. degree from Chalmers University of Technology, Göteborg, Sweden in 2006. His thesis was focused on nonlinear intrachannel signal impairments in optical fiber communications systems. In 2006, he joined the research institute IMEGO in Göteborg, Sweden, where he worked with digital signal processing for inertial navigation with MEMS-based accelerometers and gyroscopes. In 2009, he joined the Photonics

Laboratory, Chalmers University of Technology, where he currently holds a position as Assistant Professor. His research interests include nonlinear effects in optical fibers and digital signal processing in coherent optical receivers.

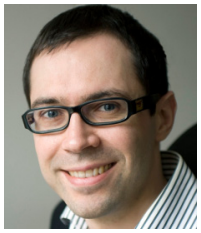

Henk Wymeersch is an Assistant Professor with the Department of Signals and Systems at Chalmers University of Technology, Sweden. Prior to joining Chalmers, he was a Postdoctoral Associate with the Laboratory for Information and Decision Systems (LIDS) at the Massachusetts Institute of Technology (MIT). Dr. Wymeersch obtained his Ph.D. degree in electrical engineering/applied sciences in 2005 from Ghent University, Belgium. In 2006, he won the Alcatel Bell Scientific Award for his Ph.D. thesis. He is a member of the IEEE, Associate Editor for *IEEE Communication Letters*, for the *Journal of Computer Systems, Networks, and Communications*, and author of *Iterative Receiver Design* (Cambridge University Press, August 2007). His research interests include algorithm design for wireless transmission, coherent optical communications, and indoor navigation.

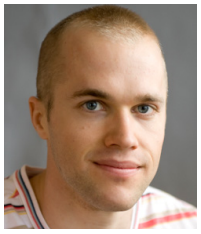

Martin Sjödin was born in Mölndal, Sweden, in 1983. He received his M.Sc. degree in engineering physics from Chalmers University of Technology, Göteborg in 2007, for which he was awarded the John Ericsson medal. In 2008, he joined the Photonics Laboratory, Chalmers University of Technology, where he is currently working toward a Ph.D. degree. His research interests include self-homodyne and intradyne optical coherent systems using advanced modulation formats.

A. Serdar Tan was born in Erzurum, Turkey, in 1982. He received his B.S. degree in electrical and electronics engineering from Middle East Technical University, Ankara, Turkey, in 2003, and his Ph.D. degree in electrical and electronics engineering from Bilkent University, Ankara, Turkey, in 2009. He worked as a Postdoctoral Researcher in Chalmers University of Technology, Sweden. His research interests include channel coding, synchronization and coherent optical communications. Dr. Tan is now with the Turkish military.

Erik Agrell received his M.Sc. degree in electrical engineering in 1989 and his Ph.D. degree in information theory in 1997, both from Chalmers University of Technology, Sweden.

From 1988 to 1990, he was with Volvo Technical Development as a Systems Analyst, and from 1990 to 1997, with the Department of Information Theory, Chalmers University of Technology, as a Research Assistant. In 1997–1999, he was a Postdoctoral Researcher with the University of Illinois at Urbana-Champaign and the University of California, San Diego. In 1999, he joined the faculty of Chalmers University of Technology, first as an Associate Professor, and since 2009 as a Professor in communication systems. His current research interests include coding, modulation, and equalization for fiber-optic channels, bit-interleaved coded modulation and multilevel coding, bit-to-symbol mappings in coded and uncoded systems, lattice theory and sphere decoding, and multidimensional geometry.

Professor Agrell served as Publications Editor for *IEEE Transactions on Information Theory* from 1999 to 2002.

Peter A. Andrekson received his Ph.D. from Chalmers University of Technology, Sweden in 1988. After about three years with AT&T Bell Laboratories, Murray Hill, NJ, USA, during 1989–1992, he returned to Chalmers, where he is now a Full Professor in the Department of Microtechnology and Nanoscience. He was Director of Research at Cenix Inc. in Allentown, PA, USA, during 2000–2003, and with the newly established Center for Optical Technologies at Lehigh University, Bethlehem, PA, USA, during 2003–2004. His research interests include nearly all aspects of high-speed and high-capacity fiber communications, such as optical amplifiers, nonlinear pulse propagation, all-optical functionalities, and very high speed transmission. He is co-founder of the optical test & measurement company PicoSolve Inc., now part of EXFO, and is Director of EXFO Sweden AB.

Andrekson is a Fellow of the Optical Society of America and a Fellow of the IEEE. He is the author and co-author of over 300 scientific publications and conference papers in the area of optical communications, more than 60 of which were invited papers at leading international conferences and journals. He is or has served on several technical program committees, including OFC and ECOC, and as international project and candidate evaluator, and has also served as an expert for the evaluation of the Nobel Prize in Physics in 1996 and in 2009. He was an associate editor for *IEEE Photonics Technology Letters* during 2003–2007. He also holds several patents. In 1993 he was awarded a prize from the Swedish government research committee for outstanding work performed by young scientists, and in 2000 he was awarded the Telenor's Nordic research award for his contribution to optical technologies.

Magnus Karlsson received his Ph.D. in 1994 from Chalmers University of Technology, Göteborg, Sweden. Since 1995, he has been with the Photonics Laboratory at Chalmers, first as an Assistant Professor and since 2003 as a Professor in photonics. He has authored or co-authored around 200 scientific journal and conference contributions and is currently an associate editor of *Optics Express*. He has served on the technical committee for the Optical Fiber Communication Conference (OFC) (in 2009 as subcommittee chair). He currently serves on the technical program committees for the European Conference of Optical Communication (ECOC) and the Asia Communications and Photonics Conference (ACP).

His research has mainly been devoted to nonlinear fiber optics and optical communications in a broad sense, from fundamental transmission effects, such as fiber nonlinearities and polarization mode dispersion, to applied issues, such as high-capacity data transmission and all-optical switching. Currently he is devoted to parametric amplification, multilevel modulation formats, and coherent transmission in optical fibers.